5421 BIOFILM GROWTH AND HYDRAULIC PERFORMANCE

KEY WORDS: Biological properties; Energy losses; Films; Fouling; Friction esistance; Hydraulic pressure; Microbes; Pipelines; Roughness; Slime; Valls; Water supply

ABSTRACT: An experimental investigation of the deleterious effect of microbial slime ayers on the hydraulic performance of water conduits is presented. The underlying echanisms that lead to an increase of frictional losses in the conduit are explored and eir relative importance is discussed. It is shown that although the slime layer is iscoelastic and filamentous, its effect on frictional resistance can be adequately epresented through an increase in rigid equivalent sand roughness of the conduit wall.

EFERENCE: Picologlou, Basil F., Zelver, Nicholas, and Characklis, William G., Biofilm Growth and Hydraulic Performance," *Journal of the Hydraulics Division*, SCE, Vol. 106, No. HY5, Proc. Paper 15421, May, 1980, pp. 733-746

JOURNAL OF THE HYDRAULICS DIVISION

BIOFILM GROWTH AND HYDRAULIC PERFORMANCE

By Basil F. Picologlou,[1] Nicholas Zelver,[2] and William G. Characklis[3]

INTRODUCTION

Biofouling in water conduits causes pronounced increases in fluid frictional resistance. The resulting energy losses are of major concern to the water-supply and power industries.

Biofouling is a general term referring to undesirable effects due to attachment of microorganisms at liquid-solid interfaces. The microorganisms produce a polysaccharide slime layer (5,6,8) that, when formed on the inside surface of water conduits, increases frictional resistance in flow systems resulting in energy losses or losses in pipeline capacity.

Deterioration of pipeline capacity attributed to biofilm development can be substantial. Seifert and Kruger (14) report a 55% reduction of original capacity in a 50-mile (80-km) long water-supply pipeline with a 23.62-in. (600-mm) ID due to a thin slimy layer approx 0.026 in. (650 μm) thick. Table 1 documents other case histories of biofouling in water-supply lines (3).

Biofouling is not limited to microbial activity. The term includes the interaction of the microorganisms and the slime layer with both the chemistry of the solid surface and the bulk fluid. These interactions can enhance some of the more commonly known fouling phenomena such as precipitation or crystallization (scaling) and corrosion. In these latter cases, the wall layer attains a much more rigid structure and the pronounced increase in frictional resistance can be successfully explained by the increase in the equivalent sand roughness of the pipe wall. In the case of microbial slime layers, the situation is more complex. The thickness and morphology of the slime layers are functions of the operating conditions. A change in operating conditions, such as an increase in wall shear stress, can cause significant changes in the morphology and thickness of the biofilm, thus changing the value of the equivalent sand roughness. In addition, the viscoelastic nature of the slime layer and its filamentous morphology suggest

Note.—Discussion open until October 1, 1980. To extend the closing date one month, a written request must be filed with the Manager of Technical and Professional Publications, ASCE. This paper is part of the copyrighted Journal of the Hydraulics Division, Proceedings of the American Society of Civil Engineers, Vol. 106, No. HY5, May, 1980. Manuscript was submitted for review for possible publication on May 18, 1979.

[1]Engr., Argonne National Lab., Argonne, Ill.
[2]Research Engr., Dept. of Civ. Engrg., Montana State Univ., Bozeman, Mont.
[3]Sr. Research Engr., Dept. of Civ. Engrg. and Adjunct Prof., Dept. of Civ. Engrg. and Chemical Engrg., Montana State Univ., Bozeman, Mont.

that perhaps additional dissipation mechanisms contribute significantly to the increased frictional resistance. Consequently, description of the biofilm effect by a unique value of equivalent sand roughness may be inadequate over the entire range of the operating conditions.

The purpose of this study is to explore some of these possibilities. This paper will only be concerned with microbial slime layers and, therefore, the term *biofouling* will be used for microbial fouling and the term *biofilm* for the microbial slime layer.

Experimental Methods

Only the salient features of the system employed are given herein. For additional information, see Refs. 16 and 4.

The experimental system was designed so that important features of full-scale operations can be simulated. Moreover, uniform biofilm attachment and spatially uniform growth conditions were deemed desirable. These considerations led

TABLE 1.—Data Summary from Case Histories of Closed Conduits Experiencing Frictional Losses due to Biofilms

Reduction in design flow capacity (1)	Biofilm thickness, in micrometers (2)	Conduit diameter, in centimeters (3)	Conduit length, in kilometers (4)	Conduit surface (5)	Reference (6)
12% in 2 yr	800	105	13	cement	9
23%	1,600	90	13	concrete	9
16% in 3 weeks	3,000	90	41	steel	1
55% in 3 yr	635	60	93	steel	15
3.5% in 1 yr	—	36	2.5	steel	7

to the development and employment of three Tubular Fouling Reactors (TFR). A detailed diagram of TFR3 is presented in Fig. 1. The TFR1 and TFR2 were essentially similar, the major difference being the use of a fermenter within the recycle loop. Other differences between these reactors were introduced for research on aspects of biofouling other than the ones reported herein. Basically, all three configurations provide a tubular reactor as part of a recycle loop. Biofilm properties and pressure drop were measured in this tubular reactor.

The glass recycle loop was designed so that: (1) Water and substrate requirements are minimized; (2) concentration gradients are minimized and the biofilm is relatively uniform, which is accomplished by employing recycle flow rates, F_R, much larger than the volumetric feed flow rates, F; and (3) the wall shear stress is independent of the mean residence time in the recycle reactor.

The recycle flow rate, F_R, measured with a cumulative flow meter, is maintained with a rotary screw pump, and the pressure drop, Δp, over a specified length of glass pipe, L, is measured either with an inclined or with a U-tube manometer.

In some of the experiments, the flow rate, F_R, was kept constant during biofilm growth while in others the wall shear stress (i.e., pressure drop Δp) was maintained constant. Pertinent dimensions and additional descriptive information for the TFR are presented in Table 2.

For the purposes of measuring the film thickness, small glass sample tubes 0.5 in. (12.7 mm) ID and 1.97 in. (50 mm) in length are introduced as an integral part of the tubular reactors. In TFR1 and TFR2 sample tubes are inserted end-to-end in an acrylic plastic test section 3/4 in. (19 mm) ID and 29.9 in. (760 mm) in length. The test section is connected to the recycle loop with pipe unions to provide easy access to the sample tubes. The TFR3 test section is similar, but the outer casing is made of stainless steel, is 39.37 in. (1,000 mm) long, and is connected with compression fittings. At designated intervals,

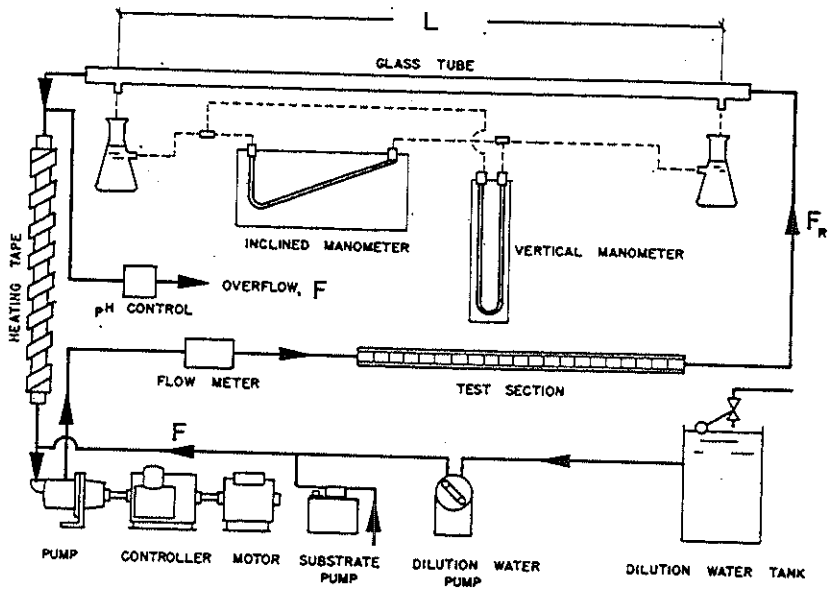

FIG. 1.—Schematic Diagram of TFR3 Experimental System

a sample tube is removed from the reactor and a clean sample tube inserted in its place. (The removal of the fouled sample tubes proceeds from the downstream to the upstream end of the test section.) The fouled sample tube is then drained to reduce excess water. Drainage time in the TFR1 and TFR2 systems is 10 min. Drainage time is reduced to 2.5 min in the TFR3 system because the film appeared to be drying around the end of the sample tube.

Biofilm volume is measured by determining its volumetric displacement as outlined in detail in Ref. 16. Wet biofilm thickness is determined by dividing biofilm volume by the surface area of the sample tube. The measurements, when performed with care, produce results with ±10% margin of error. The measured film thickness is a function of the drainage time and can be as much as 36% larger for drainage times of 2.5 min than it is for drainage times of 10 min.

Results

Frictional Resistance.—Increase in fluid frictional resistance due to biofilm accumulation during constant flow-rate experiments (TFR1 and TFR2) causes an increase in pressure drop and power requirements for pumping as shown in Fig. 2 for a typical experiment.

Conversely, if pressure drop is held constant (TFR3), flow capacity is reduced.

TABLE 2.—Pertinent Dimensions of TFR

Dimensions (1)	TFR1 (2)	TFR2 (3)	TFR3 (4)
Liquid volume, in cubic centimeters	6,719	4,500	2,100
Wetted area, in square centimeters	10,750	7,600	3,470
Tube length, in centimeters	2,194	1,755	869
Inside tube diameter, in centimeters	1.27	1.27	1.27
Volumetric feed rate, in cubic centimeters per minute	440	300	140 (TFR3-1 to TFR3-4) 280 (TFR3-5 to TFR3-16)
Mean hydraulic retention time, in minutes	15	15	15 (TFR3-1 to TFR3-5) 7.5 (TFR3-5 to TFR3-16)
Test section			
length, in centimeters	76	76	100
inside diameter, in centimeters	1.9	1.9	1.95
outside diameter, in centimeters	2.3	2.3	2.3
Sample tubes			
number	14	42	22
length, in centimeters	5	5	5
inside area of tube wall, in square centimeters	20	20	20
volume of tube wall, in cubic centimeters	8.824	8.824	8.824
Length for ΔP, in centimeters	232	232	120

Fig. 3 shows a typical experimental curve in which flow capacity was reduced to 42% of the original capacity in a 100-h laboratory experiment.

Frictional resistance can be represented by a dimensionless friction factor given by (12)

$$f = 2.0 \frac{d}{L} \frac{\Delta P}{\rho_w \bar{v}^2} \quad \ldots\ldots\ldots\ldots\ldots\ldots\ldots\ldots\ldots\ldots\ldots\ldots\ldots\ldots (1)$$

in which f = friction factor; d = tube diameter; ρ_w = fluid density; $\bar{v}$ = average fluid velocity; ΔP = pressure drop along length L; and L = length between pressure ports.

The change in friction factor with time for a TFR3-7 experiment is shown in Fig. 4; the measured biofilm thickness for the same experiment is also indicated.

The friction factor is related to the Reynolds number and the equivalent sand roughness, k_s, through the empirical Colebrook-White equation (12). This equation provides good correlation for friction factor versus Reynolds number for various "commercially rough" pipes throughout the hydraulically smooth, transition, and fully rough regimes. The Colebrook-White equation, solved for the equivalent sand roughness, k_s, yields

$$k_s = \frac{d}{2}\left(10^{(0.87-0.50/f^{1/2})} - \frac{18.70}{R f^{1/2}}\right) \quad \ldots\ldots\ldots\ldots\ldots\ldots\ldots\ldots\ldots\ldots\ldots\ldots (2)$$

in which d = tube diameter; $R = \bar{v}d/\nu$ = Reynolds number; $\bar{v}$ = mean fluid velocity; and ν = kinematic viscosity. This expression can be used to compute an equivalent sand roughness for the biofilm from a measurement of the flow rate, R, and pressure drop, f.

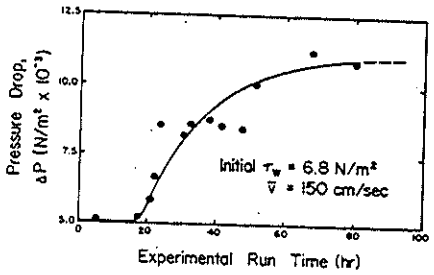

FIG. 2.—Change in Pressure Drop with Time for Experiment (TFR1-12) Conducted at Constant Average Velocity

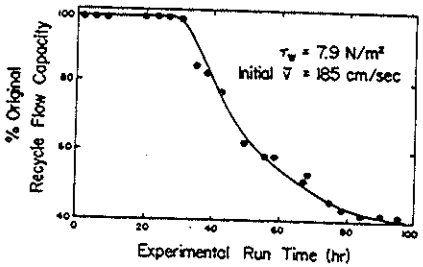

FIG. 3.—Change in Volumetric Flow Rate in Recycle Tube with Time for Experiment (TFR3-5) Conducted at Constant Pressure Drop

In all TFR experiments, k_s increases with time; Fig. 5 shows the progression of k_s with time for a typical experiment. Fig. 6 indicates the dependence of k_s on biofilm thickness for the range of shear stress investigated [0.943×10^{-3} psi–1.146×10^{-3} psi (6.5 N/m²–7.9 N/m²)].

Determination of the flow regime (smooth, transitional, or fully rough) depends on the magnitude of k_s relative to the size of the viscous sublayer (δ_l); δ_l is given by (12)

$$\delta_l = \frac{10d}{R}\left(\frac{f}{2}\right)^{-0.5} \quad \ldots\ldots\ldots\ldots\ldots\ldots\ldots\ldots\ldots\ldots\ldots\ldots\ldots\ldots (3)$$

More specifically, when $k_s < \delta_l$, the pipe is considered hydraulically smooth; when $14\delta_l > k_s > \delta_l$, the flow is in the transitional regime; when $k_s > 14\delta_l$, the flow is in the fully rough regime (12).

In all TFR experiments (except TFR3-11, which employed a preroughened tube), the flow regime, as determined from the preceding criteria, progresses from hydraulically smooth to transitional or fully rough.

Analysis

The results indicate that frictional resistance due to biofilm accumulation can be substantial. The following mechanisms, which can contribute to this pronounced increase in frictional resistance, have been considered: (1) Reduction in available tube cross section due to biofilm accumulation; (2) change in fluid viscosity due to presence of dissolved macromolecules generated by the biofilm; (3) viscous dissipation within the biofilm due to its creeping flow in the downstream direction; (4) viscous dissipation within the biofilm, due to its viscoelastic nature, as a result of oscillations set up by the turbulent flow; (5) increased dissipation in the fluid due to increased surface roughness as a result of biofilm accumulation; and (6) increased dissipation in the fluid due to presence of biofilm filaments.

Pressure Drop due to Tube Constriction.—Constriction of the tube due to biofilm accumulation cannot, alone, account for the increase in frictional resistance as shown in Fig. 7. Fig. 7 indicates: (1) The increase in pressure drop and biofilm thickness with time for a typical experiment (TFR1-12); and (2) the increase in pressure drop for a decrease in radius equal to the measured biofilm thickness as calculated from the Blasius equation for a smooth tube (11):

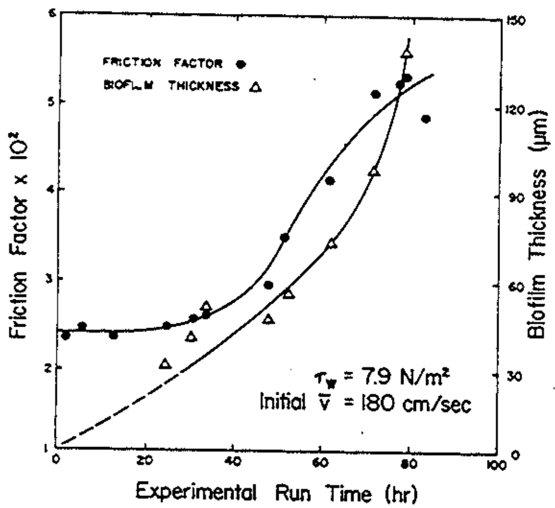

FIG. 4.—Change in Friction Factor and Biofilm Thickness with Time for Experiment (TFR3-7) Conducted at Constant Pressure Drop

$$f = \frac{0.316}{\left(\frac{d\bar{v}}{\nu}\right)^{0.25}} \qquad (4)$$

Constriction of the tube accounts for an approximate 10% increase in pressure drop whereas pressure drop due to biofilm accumulation increases approx 110%.

Clearly, the effect of a reduction in tube diameter by biofilm accumulation is minimal.

Fluid Viscosity.—Fluid viscosity did not change during a TFR experiment. Fluid viscosity from TFR experiments under different conditions was measured using a capillary viscometer. Fluid viscosity never varied more than 2.0% from that of water.

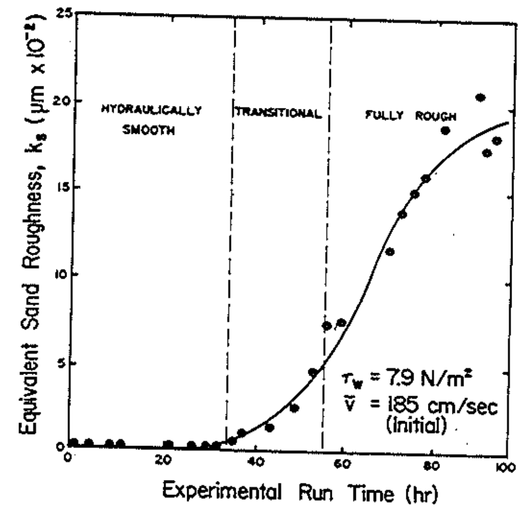

FIG. 5.—Change in Equivalent Sand Roughness with Time for Experiment (TFR3-5) Conducted at Constant Pressure Drop

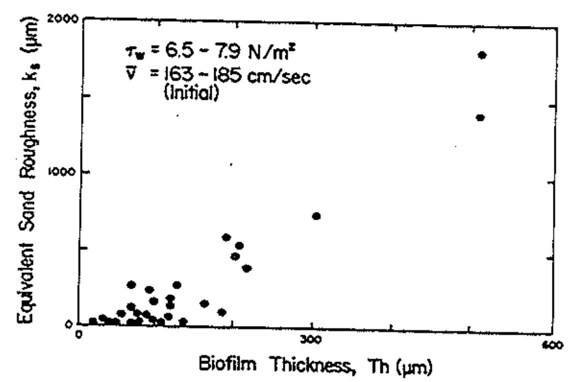

FIG. 6.—Change in Calculated Equivalent Sand Roughness with Biofilm Thickness for All Experiments Conducted at Constant Pressure Drop

Viscous Dissipation within Biofilm due to Its Creeping Flow in Downstream Direction.—Brauer (2) performed experiments on form stability of the interior of asphalt-lined pipes as a function of temperature of the flowing water. At higher temperatures, the asphalt coating assumed a rippled surface structure

that was acompanied by an unusual increase in frictional resistance. Brauer explained the phenomenon as an actual flow of the coating under the action of shear stresses. Energy is dissipated by the asphalt being dragged along the pipe surface.

Transport of biofilm in the TFR system seems an unlikely explanation for the high frictional resistance in the fouled TFR system for the following reasons: (1) The biofilm coating always appeared uniform throughout the system (biofilm transport would require a steady supply of film or else the wall coating would disappear); and (2) there was no evidence of an accumulation of biofilm in pipe bends or other areas where film could collect (biofilm transport would result in accumulation of film as film flowed to the downstream end of a tube).

Viscous Dissipation within Biofilm due to Its Oscillatory Response to Turbulent-Flow Excitation.—Rheological measurements performed on biofilm grown on

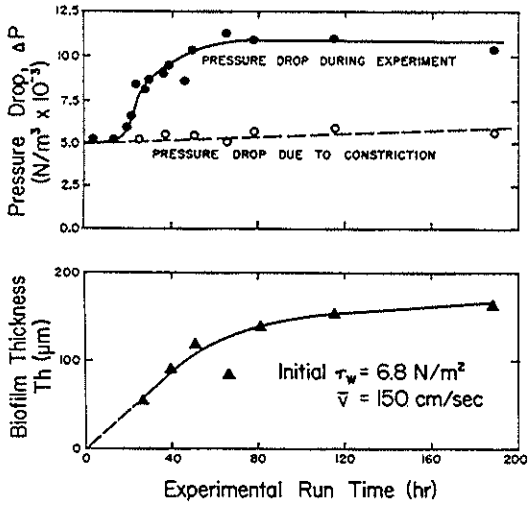

FIG. 7.—Measured Pressure Drop Compared to Calculated Pressure Drop due to Decrease in Tube Radius Equivalent to Biofilm Thickness (TFR1-12)

platens of a Weissenberg Rheogoniometer established the viscoelastic nature of the biofilm (16). As a result of the relatively large viscous modulus (the viscous modulus was larger than the elastic modulus at all frequencies tested between 7 Hz and 12 Hz), the possibility exists that the biofilm draws energy from the flow, such energy being eventually dissipated through viscous action. The situation is quite complex and defies analysis, particularly since there is a nonlinear coupling between the structure of the turbulent flow and the biofilm response. Since the total losses can quite satisfactorily be attributed to increased film surface roughness, one can indirectly argue that any dissipation within the biofilm is of secondary importance.

Increased Dissipation in Fluid due to Increased Surface Roughness as Result of Biofilm Accumulation.—Frictional resistance of biofilms grown under constant pressure drop (TFR3) have been compared to the frictional resistance of pipes

with a rigid roughness as given by the Colebrook-White equation. The following are indicated: (1) Frictional resistance due to biofilm shows a similar dependency on Reynolds number as frictional resistance due to commercially rough pipe surface; (2) frictional resistance is dependent on biofilm thickness; and (3) frictional resistance does not increase above the hydraulically smooth pipe value until a critical biofilm thickness is obtained.

The Blasius-Stanton or Moody diagram (10) can be used to compare frictional resistance due to biofilm with frictional resistance of rigid rough surfaces. The Blasius-Stanton diagram is a plot of friction factor versus Reynolds number for a series of pipes with different equivalent sand roughness; the friction factor in a pipe with a rigid rough surface depends on both the relative roughness and the Reynolds number.

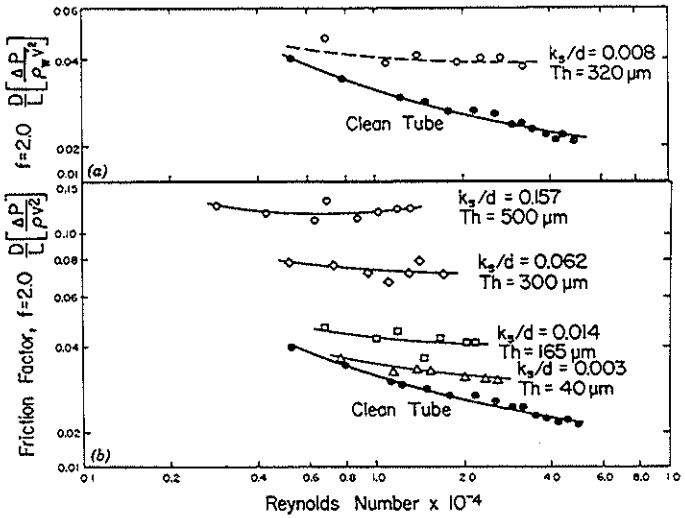

FIG. 8.—Change in Friction Factor as Function of Reynolds Number and Roughness: (*a*) Due to Biofilm Formation (TFR3-16); (*b*) At Different Stages of Biofilm Development (TFR3-5)

The relationship between friction factor and Reynolds number for the fouled TFR3 system is presented in Fig. 8(*a*). This figure shows the dependency of friction factor on Reynolds number is the same as for a tube with a rigid rough surface between the range of Reynolds numbers investigated (5,000–48,000). These data were obtained by reducing in steps the shear stress from its initial value in a given experiment and calculating friction factor and Reynolds number at each step. Reduction, rather than increase of the shear stress from the initial condition, minimized sloughing of biofilm during an experiment.

Fig. 8(*b*) shows friction factor versus Reynolds number for a TFR3 experiment at different stages of biofilm development; friction factor increases with biofilm thickness. The relationship between biofilm thickness and friction factor for all experiments at wall shear stress from 0.943×10^{-3}psi–1.146×10^{-3} psi

(6.5 N/m^2–7.9 N/m^2) is shown in Fig. 9(*a*); friction factor is dependent on film thickness after a critical thickness (TH_{crit}) approximately equal to the thickness of the viscous sublayer is attained.

The critical film thickness corresponds to the stage of biofilm development of which surface irregularities protrude through the viscous sublayer. Until this stage, the roughness peaks are smaller than the viscous sublayer thickness ($k_s < \delta_l$) and the friction factor does not increase (the tube is hydraulically smooth). For a wall shear stress of 0.943×10^{-3} psi–1.146×10^{-3} psi (6.5 N/m^2–7.9 N/m^2) the viscous sublayer is approximately equal to 0.0016 in. (40 m); this corresponds well with the observed TH_{crit} 0.0012 in.–0.0014 in. (30 μm–35 μm) for the same wall shear-stress range. This is shown in Fig. 9(*b*), which expands the initial fouling stage of Fig. 9(*a*).

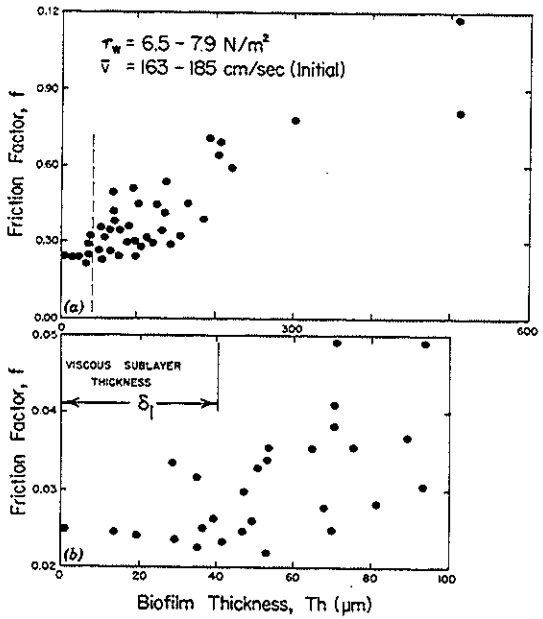

FIG. 9.—Change in Friction Factor with Biofilm Thickness: (*a*) In Experiments Conducted at Constant Pressure Drop; (*b*) For Constant Pressure-Drop System, Indicating Viscous Sublayer Thickness

If the biofilm indeed increases the effective roughness of the tube wall, a dependency of calculated equivalent sand roughness, k_s on biofilm surface morphology should be expected. It has been well established that different surface roughness configurations having identical sizes of roughness peaks result in different equivalent sand roughness (12). The results of this investigation suggest that the equivalent sand roughness produced by the biofilm is of the order of magnitude of the biofilm thickness.

Indeed, Fig. 6 (k_s versus biofilm thickness) shows that the equivalent sand roughness is dependent on biofilm thickness for all TFR3 experiments at a fluid shear stress of 0.943×10^{-3} psi–1.146×10^{-3} psi (6.5 N/m^2–7.9 N/m^2).

The data imply that the equivalent sand roughness of the biofilm can be greater than the actual film thickness. Furthermore, scatter in the k_s data cannot be attributed to change in feed glucose flux or change in temperature (30° C to 35° C). The difficulty in determining the dependency of k_s on biofilm thickness may be due to one or all of the following reasons:

1. The biofilm thickness measurement is an average thickness measurement and does not measure actual height of roughness peaks. The average biofilm thickness could be less than any roughness peaks of the biofilm.
2. Drainage of the sample tube prior to the biofilm thickness measurement may decrease the biofilm volume and thus decrease the biofilm thickness; the

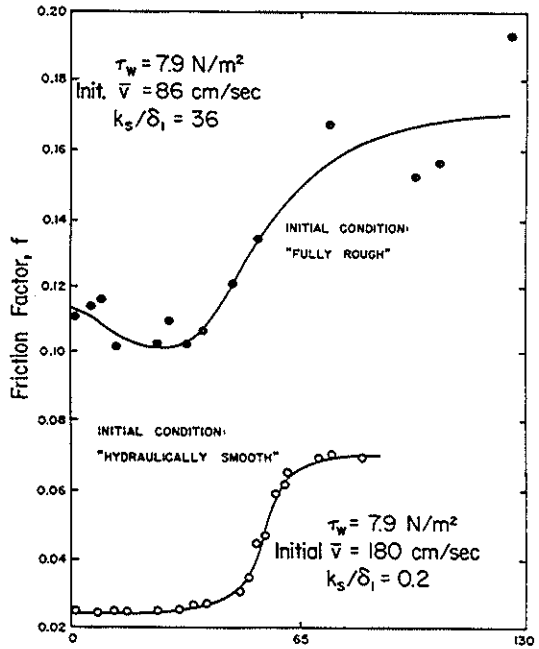

FIG. 10.—Comparison of Friction Factor Progression in Preroughened Tube (TFR3-11) with That in Initially Smooth Tube (TFR3-6)

effective biofilm thickness may be greater with the sample tube in-situ and the biofilm saturated with water.

3. As mentioned previously, the equivalent sand roughness depends on the roughness peaks, but it is not numerically equal to their size. It is not unusual for the equivalent sand roughness to be greater than the roughness peaks (12).

In turbulent flow in conduits with compliant boundaries the possibility exists that when the Reynolds number exceeds a certain value, rippling of the compliant boundary takes place accompanied by drastic changes in friction factor (13). Such a phenomenon would manifest itself, according to the preceding analysis,

as a significant change in the equivalent sand roughness for the biofilm. Such transitions were not observed in our experiments for the range of Reynolds numbers investigated. A single equivalent sand roughness was sufficient to correlate the friction factor and the Reynolds number.

Although the frictional resistance effects of biofilm can be adequately described by formulas suitable for rigid rough surfaces, the conclusion should not be drawn that, indeed, the biofilm presents a rigid rough surface to the flow. Such a notion is an oversimplification and cannot account for all experimental observations, e.g., Fig. 10 compares two TFR3 experiments with identical conditions except for the roughness of the inner tube surface. The surface of TFR3-6 is initially hydraulically smooth ($k_s/\delta_l = 0.20$) while for TFR3-11 the surface is initially fully rough ($k_s/\delta_l = 36$); the fully rough condition is due to sand grains [average diameter of 0.0087 in. (00.22 mm)] immobilized

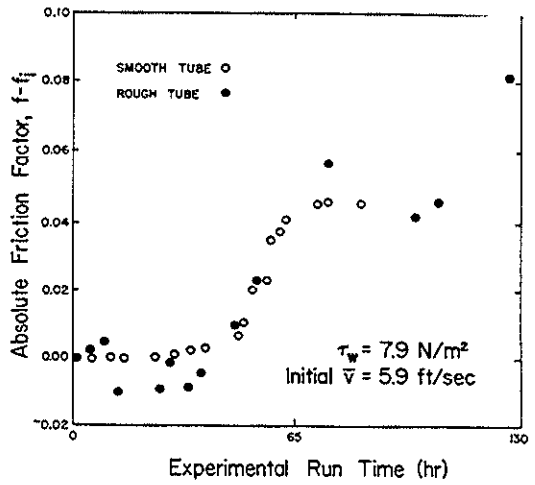

FIG. 11.—Friction-Factor Change (f-f_i) in Preroughened Tube (TFR3-11) and in Smooth Tube (TFR3-6)

on the inside surface. The following results are evident: (1) Initial friction factor, f_i, is greater in the rough tube and frictional resistance remains greater at all times; and (2) frictional resistance is reduced slightly during the first 30 h in the rough tube.

The decrease in frictional resistance at the beginning of TFR3-11 suggests that the biofilm developed between the sand grains and provided a less rough surface up to approx 30 h.

The friction factor increases relative to the clean conditions, $f - f_i$, for each experiment are superimposed in Fig. 11 and indicate little difference. The additional pronounced frictional resistance in the preroughened tube indicates that the effect of the biofilm on frictional resistance is not due to a simple increase of rigid surface roughness. A possible explanation may lie with the fact that a significant amount of the frictional loss is due to the presence of the biofilm filaments. If so, growth of biofilm filaments on a fully rough pipe

will increase the losses and increase the friction factor to the same extent observed in an initially smooth pipe.

Increased Dissipation in Fluid due to Presence of Biofilm Filaments.—The filaments of the biofilm were observed to flutter with a frequency that is a function of the average fluid velocity. It was also observed that frictional resistance increased with increasing filament length. Such increases are analogous to increased drag in streams due to bottom vegetation. Similar phenomena occur in the study of atmospheric boundary layers due to the presence of grassy vegetation.

Our observations (experiments with the rough tubes and the casual observations linking filament length to frictional resistance) suggest that a significant portion of the frictional resistance is to be attributed to the action of the filaments. More research is needed to quantify this effect.

Conclusions

The objective of this study was to obtain fundamental information on increased frictional resistance due to biofilms in water conduits.

The following conclusions are derived using a laboratory, circular tube reactor:

1. Increase in frictional resistance corresponds to an increase in biofilm thickness or biofilm mass.
2. Increase in the calculated equivalent sand roughness corresponds to an increase in biofilm thickness.
3. Increase in frictional resistance is characterized by an induction period at small biofilm thicknesses followed by a rapid increase after film thickness reaches a critical value. The critical film thickness corresponds to the viscous sublayer thickness [0.0016 in. (40 μm)] at a fluid shear stress of 1.146×10^{-3} psi (7.9 N/m^2). Measured biofilm thickness varied from 0.0004 in.–0.04 in. (10 μm–1,000 μm).
4. Constriction of the tube due to biofilm production accounts for only approx 10% of the frictional resistance.
5. The effect of Reynolds number on friction factor (e.g., Moody Diagram) for a tube with an attached biofilm is similar to a tube with a rigid rough surface in the range of Reynolds numbers investigated (5,000–48,000).
6. The filamentous nature of the biofilm contributes to the increase in frictional resistance.

Acknowledgments

The writers gratefully acknowledge the following: Support from the National Science Foundation (ENG 74-11957 and ENG 77-26934) and the Electric Power Research Institute (902-1); manuscript preparation by Maurine Lee and Linda Graetz; graphics by Duane Marks. L. V. McIntire provided helpful comments throughout the study. The work was done at Rice University, Houston, Tex.

Appendix I.—References

1. Arnold, G. E., "Crenothrix Chokes Conduits," *Engineering News Record*, Vol. 116, 1963, pp. 774–775.

2. Brauer, H., "Flow Resistance in Pipes with Ripple Roughness," *Chemische Zeitung*, Vol. 87, 1963, pp. 199–210.
3. Characklis, W. G., "Attached Microbial Growths. II. Frictional Resistance Due to Microbial Slimes," *Water Research*, Vol. 7, 1973, pp. 1249–1259.
4. Characklis, W. G., "Biofouling Film Development and Destruction," *Final Report*, Project No. 902-1, Electric Power Research Institute, Palo Alto, Calif., 1979
5. Corpe, W. A., "An Acid Polysaccharide Produced by a Primary Film-Forming Marine Bacterium," *Developments in Industrial Microbiology*, Vol. 12, 1970, pp. 402–412.
6. Costerton, J. W., Geesey, G. G., and Cheng, K. J., "How Bacteria Stick," *Scientific American*, Vol. 238, 1978, pp. 86–95.
7. Derby, R. L., "Control of Slime Growth in Transmission Lines," *Journal of American Water Works Association*, Vol. 39, 1947, pp. 1107–1114.
8. Fletcher, M., and Floodgate, G. D., "An Electron Microscopic Demonstration of an Acidic Polysaccharide in the Adhesion of a Marine Bacterium to Solid Surfaces," *Journal of General Microbiology*, Vol. 74, 1973, pp. 325–334.
9. Minkus, A. J., "Determination of the Hydraulic Capacity of Pipelines," *Journal of New England Water Works Association*, Vol. 68, 1954, pp. 1–10.
10. Moody, L. F., "Friction Factors for Pipe Flow," *Transactions of the American Society of Mechanical Engineers*, Vol. 66, 1944, pp. 671–684.
11. Olson, R. M., *Essentials of Engineering Fluid Mechanics*, Intext Educational Publishers, New York, N.Y., 1973.
12. Schlichting, H., *Boundary Layer Theory*, McGraw-Hill Book Co., New York, N.Y., 1968.
13. Schuster, H., "Fluid Friction in the Presence of Non-rigid Boundaries," thesis presented to Johns Hopkins University, at Baltimore, Md., in 1971, in partial fulfillment of the requirements for the degree of Doctor of Philosophy.
14. Seifert, L., and Kruger, W., "Unusual High Friction Factor in a Long Water Supply Line," *Verein Deutscher Ingenieure Zeitschrift*, Vol. 92, 1950, pp. 189–191.
15. Widerhold, W., "Effect of Wall Deposits on Hydraulic Loss in Pipelines," *Gas Wass Fach.*, Vol. 90, 1949, pp. 634–641.
16. Zelver, N., "Biofilm Development and Associated Energy Losses in Water Conduits," thesis presented to Rice University, at Houston, Tex., in 1979, in partial fulfillment of the requirements for the degree of Master of Science.

Appendix II.—Notation

The following symbols are used in this paper:

d = tube diameter;
f = friction factor (dimensionless);
f_i = initial friction factor (dimensionless);
k_s = equivalent sand roughness;
L = tube length across which pressure drop is measured;
R = Reynold's number (dimensionless);
Th = biofilm thickness;
Th_{crit} = biofilm thickness at which frictional resistance begins to increase;
$\bar{v}$ = average fluid velocity;
ΔP = pressure drop;
δ_l = thickness of viscous sublayer;
ν = kinematic viscosity;
ρ_w = density of water; and
τ_w = wall shear stress.